



OPEN

CRISPR-based transcriptional activation tool for silent genes in filamentous fungi

László Mózsik^{1,6}, Mirthe Hoekzema^{1,5,6}, Niels A. W. de Kok¹, Roel A. L. Bovenberg^{2,3}, Yvonne Nygård^{1,2,4} & Arnold J. M. Driessen¹✉

Filamentous fungi are historically known to be a rich reservoir of bioactive compounds that are applied in a myriad of fields ranging from crop protection to medicine. The surge of genomic data available shows that fungi remain an excellent source for new pharmaceuticals. However, most of the responsible biosynthetic gene clusters are transcriptionally silent under laboratory growth conditions. Therefore, generic strategies for activation of these clusters are required. Here, we present a genome-editing-free, transcriptional regulation tool for filamentous fungi, based on the CRISPR activation (CRISPRa) methodology. Herein, a nuclease-defective mutant of Cas9 (dCas9) was fused to a highly active tripartite activator VP64-p65-Rta (VPR) to allow for sgRNA directed targeted gene regulation. dCas9-VPR was introduced, together with an easy to use sgRNA “plug-and-play” module, into a non-integrative AMA1-vector, which is compatible with several filamentous fungal species. To demonstrate its potential, this vector was used to transcriptionally activate a fluorescent reporter gene under the control of the *penDE* core promoter in *Penicillium rubens*. Subsequently, we activated the transcriptionally silent, native *P. rubens* macrophorin biosynthetic gene cluster by targeting dCas9-VPR to the promoter region of the transcription factor *macR*. This resulted in the production of antimicrobial macrophorins. This CRISPRa technology can be used for the rapid and convenient activation of silent fungal biosynthetic gene clusters, and thereby aid in the identification of novel compounds such as antimicrobials.

Abbreviations

BGC	Biosynthetic gene cluster
CRISPRa	CRISPR activation
SM	Secondary metabolite
cDNA	Complementary DNA
sgRNA	Chimeric single guide RNA
RNPs	Ribonucleoprotein complexes
NLS	Nuclear localization signal
CP	Core promoter
TSS	Transcription start site

Fungi are amongst the most proliferous producers of secondary metabolites (SMs). These molecules, while not intrinsically required for survival, provide a biological advantage to their host¹. Many fungal SMs are beneficial to humankind and have a wide range of applications in human and animal healthcare (e.g. as antibiotics or immunosuppressants), food, agricultural and industrial sectors^{2,3}. On the other hand, SMs can be toxic and some SMs contribute to the pathogenicity of fungi while others contaminate food and crops⁴. Genes involved in secondary metabolism are often arranged in clusters, so-called biosynthetic gene clusters (BGCs), and these

¹Molecular Microbiology, Groningen Biomolecular Sciences and Biotechnology Institute, University of Groningen, Nijenborgh 7, 9747 AG Groningen, The Netherlands. ²DSM Biotechnology Center, Alexander Fleminglaan 1, 2613 AX Delft, The Netherlands. ³Synthetic Biology and Cell Engineering, Groningen Biomolecular Sciences and Biotechnology Institute, University of Groningen, Nijenborgh 7, 9747 AG Groningen, The Netherlands. ⁴Division of Industrial Biotechnology, Department of Biology and Biological Engineering, Chalmers University of Technology, Kemivägen 10, 412 96 Gothenburg, Sweden. ⁵Division of Forest Pathology, Department of Forest Mycology and Plant Pathology, Swedish University of Agricultural Sciences, Almas allé 5, 756 51 Uppsala, Sweden. ⁶These authors contributed equally: László Mózsik and Mirthe Hoekzema. ✉email: a.j.m.driessen@rug.nl

are typically regulated by pathway-specific transcription factors. As more fungal genomes, and bioinformatics tools and databases (e.g. fungal antiSMASH⁵, MIBiG⁶) have become available for the prediction, annotation and prioritization of fungal BGCs, it has become clear that filamentous fungi have an even larger biosynthetic potential than previously anticipated.

Most of the BGCs are transcriptionally silent under laboratory growth conditions, therefore products of these clusters remain elusive⁷. Various methodologies have been developed for the activation of silent BGCs, including manipulation of both BGC specific as well as global transcriptional regulators, promoter-exchange, and heterologous expression in suitable host systems [reviewed in⁸]. Marker-free genome editing remains challenging, and with only a limited number of fungal selection markers available, extensive genome manipulations is a laborious task.

The bacterial CRISPR/Cas systems have emerged as versatile biotechnological tools^{9,10}, and next to genome editing it can provide a promising alternative approach for transcriptional activation in fungi. CRISPR/Cas systems consist of only two components; a Cas nuclease and a programmable guide RNA. In case of the popular Cas9 system from *Streptococcus pyogenes* the protein can be guided to a genomic locus in a sequence-specific manner, using a single guide RNA (sgRNA) which consist of a short targeting crRNA sequence and the scaffold tracrRNA sequence. Methods for Cas9-based genome editing have been established in various filamentous fungal species [Reviewed^{11,12}], including the industrially relevant fungi *Penicillium rubens*^{13,14} (formerly identified as *P. chrysogenum*¹⁵). Cas9 and sgRNA delivery strategies include vector-based expression or genomic integration of transcriptional units encoding Cas9 and sgRNA. Alternatively, only Cas9 is expressed and the sgRNA is provided by a transformation of in vitro transcribed RNA, or both Cas9 and sgRNA are provided as pre-assembled ribonucleoprotein complexes (RNPs). The CRISPR/Cas9 genome editing tools established in filamentous fungi can edit the genome at a single as well as at multiple locations, and have effectively been applied in industrial fungi to improve compound production^{11,12}.

Beyond genome editing, CRISPR/Cas can be used as a platform for RNA guided DNA-protein interactions, and thereby deliver various effector domains to a specific genomic location. By introducing point mutations into the two nucleolytic domains, nuclease deficient versions of Cas9, called dead Cas9 (dCas9), were created¹⁶. Because dCas9 binds in a sequence-specific manner, but does not cleave DNA, it can be used for transcriptional regulation^{17,18}, epigenome editing^{19,20}, visualization of specific genomic loci²¹ and base editing²² in various eukaryotic species. For CRISPR/Cas mediated transcriptional activation (CRISPRa) several activating effector domains have been fused to dCas9 [reviewed in^{23,24}]. The often-used VPR system consists of a three-component complex, four copies of the herpes simplex VP16 transactivation domain, the transactivation domain of nuclear factor kappa B, and Epstein-Barr virus R transactivator, VP64-p65-Rta, respectively¹⁶. dCas9-VPR fusions have been successfully employed for upregulation of reporter and/or endogenous genes in mammalian cells¹⁶, in diploid²⁵ and polyploid²⁶ *Saccharomyces cerevisiae*, *Yarrowia lipolytica*²⁷, *Candida albicans*²⁸, and most recently also in the filamentous fungus *Aspergillus nidulans*²⁹.

Here we report on the implementation of a dCas9-VPR-based, genome editing free system for transcriptional activation system in the filamentous fungus *Penicillium rubens*. We successfully utilized the CRISPRa tool to activate the cryptic macrophorin BGC, resulting in production of compounds with antimicrobial activity.

Results

Construction of a fungal CRISPRa tool. CRISPR/Cas mediated gene expression activation (CRISPRa) requires a catalytically dead CRISPR-associated protein (dCas) fused to an activation domain, as well as a sgRNA to guide it to the desired locus. Here, the widely utilized fusion of dCas9 from *Streptococcus pyogenes* to the tripartite activator, VP64-p65-Rta (VPR)¹⁶ was selected for activation. For easy implementation of CRISPRa in a broad range of filamentous fungi, we constructed an AMA1-based vector for expression of the NLS tagged dSpCas9-VPR under the 40S ribosomal protein S8 promoter (*p40S*) (Fig. 1a). The AMA1 sequence -originally isolated from *A. nidulans*- allows for autonomous vector replication in several filamentous fungal species^{30,31}, and is often employed for Cas9 and sgRNA expression in gene-editing approaches in these organisms^{11,13,32,33}. The AMA1 vector was also used to supply the sgRNA, establishing CRISPRa after a single transformation. The sgRNA was expressed from the constitutive *gpdA* promoter and flanked by hammerhead (HH) and hepatitis delta virus (HDV) ribozymes to ensure defined ends for sgRNA processing and optimal functionality (Fig. 1a)³⁴.

Target specificity is determined by the sgRNA, thus by exchanging the sgRNA sequence different genes can be targeted for upregulation. To enable convenient and efficient exchange of sgRNA target sequences a sgRNA “plug-and-play” module was introduced into the AMA1 shuttle vector to facilitate cloning steps in *Escherichia coli* (Fig. 1a,b). This vector, which is the parent to all sgRNA expressing vectors, is called pLM-AMA18.0-dCas9-VPR (referred to as pAMA18.0) and also functions as a negative (non-targeting sgRNA) control. The sgRNA “plug-and-play” module works as follows; the chimeric sgRNA backbone sequence and the HDV ribozyme are already supplied on the AMA1-vector together with a *lacZ* gene flanked by BsaI restriction sites. The 20 nt spacer sequence defining the genomic target is supplied on a separate dsDNA molecule, together with the hammerhead ribozyme (HH) which includes the necessary 6 bp inverted repeat of the 5'-end of the spacer to complete the HH cleavage site. This dsDNA molecule can simply be created by PCR using two overlapping oligonucleotides (Fig. 1b) or alternatively ordered as chemically synthesized dsDNA. The fragment can then be inserted into pAMA18.0 using the Golden Gate cloning and the BsaI restriction sites³⁵. As this removes the *lacZ* gene, positive bacterial clones can easily be detected with blue-white screening. After positive sequence verification and vector extraction, the created CRISPRa vector can be introduced into the filamentous fungi of choice (Fig. 1b).

Proof of principle: activating penDE-CP_DsRed. In order to test if expression of dCas9-VPR and the sgRNA from the CRISPRa vector could activate transcription of a silent gene, we targeted dCas9-VPR to the

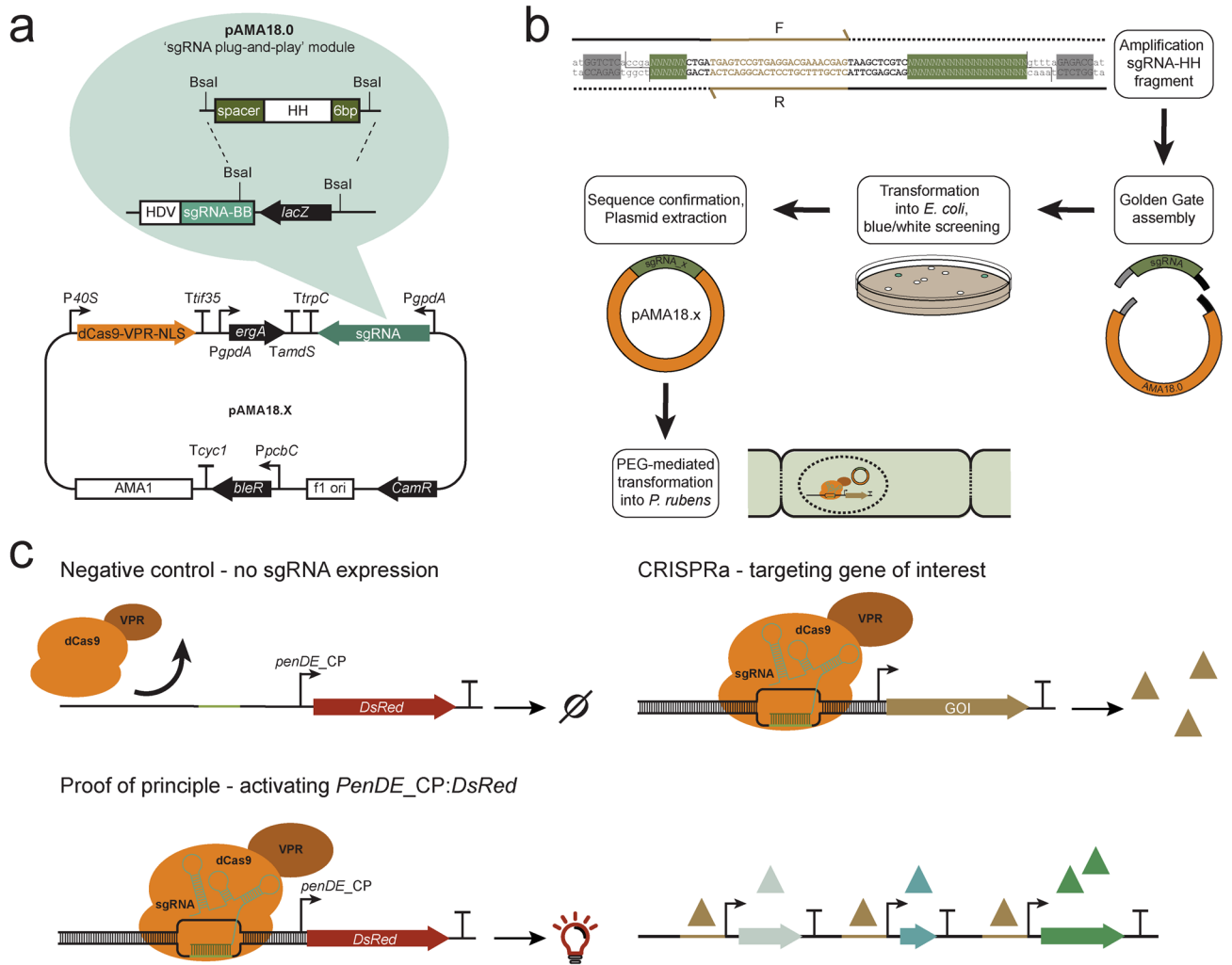


Figure 1. Overview of the programmable CRISPR/Cas-based transcriptional activation system implemented in *P. rubens*. **(a)** Schematic representation of the pAMA18.X-vector encoding the components of the CRISPR/Cas activation system, namely the dCas9-VPR and the ribozyme self-cleaved sgRNA. pAMA18.0 is the parent vector of all sgRNA containing vectors and contains the sgRNA "plug-and-play" module which is highlighted. **(b)** Diagram depicting the cloning strategy for insertion of the PCR amplified sgRNA into pAMA18.0. **(c)** CRISPRa proof of principle. In the control strain carrying pAMA18.0 no sgRNAs are transcribed, so while dCas9-VPR is present it is not targeted to a specific locus and no transcriptional activation occurs. Correct targeting of the dCas9-VPR complex to the silent *penDE-CP* is leading to *DsRed* fluorescent protein expression and hence increased fluorescence. In the same fashion when dCas9-VPR is targeted to a promoter driving a gene of interest, this results in product formation. When the targeted promoter drives a transcriptional regulator this can result in activation/repression of multiple other genes, including entire BGCs.

penDE core promoter (*penDE-CP*). The 200 bp long *penDE-CP* has previously been shown to be functional, but insufficient to drive expression on its own³⁶. For easy visualization of CRISPR based transcriptional activation, the *penDE-CP* was set to drive *DsRed-T1-SKL*, a red fluorescent reporter gene with peroxisomal targeting signal (Fig. 1c). The *penDE-CP_DsRed* reporter unit was integrated into the penicillin-locus of the *P. rubens* DS68530 (Δ penicillin-BGC), utilizing CRISPR/Cas9 ribonucleoprotein (RNP) facilitated co-transformation^{13,14} (Supplementary Fig. S1a).

Different pAMA18.0 derived vectors (pAMA18.a-f) expressing sgRNAs targeting loci +1 to -118 bp relative to the transcription start site (TSS) of the *penDE-CP* (Fig. 2a, Supplementary Fig. S2a, Supplementary Table S1) were transformed into *P. rubens* DS68530_ *penDE-CP_DsRed* and strains were analyzed using fluorescence microscopy (Fig. 2b). Increased fluorescence intensity was seen in strains transcribing *penDE-sgRNA_c*, *_d*, and *_e* but not in strains transcribing *penDE-sgRNA_a*, *_b* and *_f*. The DS68530_ *penDE-CP_DsRed* strain carrying the pAMA18.0 negative control vector which did not express any sgRNA, showed only a minimal amount of fluorescence. *DsRed* expression was also evaluated using qPCR, showing the most efficient activation for *penDE-sgRNA_c* (Fig. 2c). These results confirm that activation of *DsRed* expression was CRISPRa dependent.

To assess the performance of the different sgRNA target sequences, the BioLector microbioreactor system was used with online monitoring of scattered light (biomass) and red fluorescence intensity (Fig. 2d, Supplementary

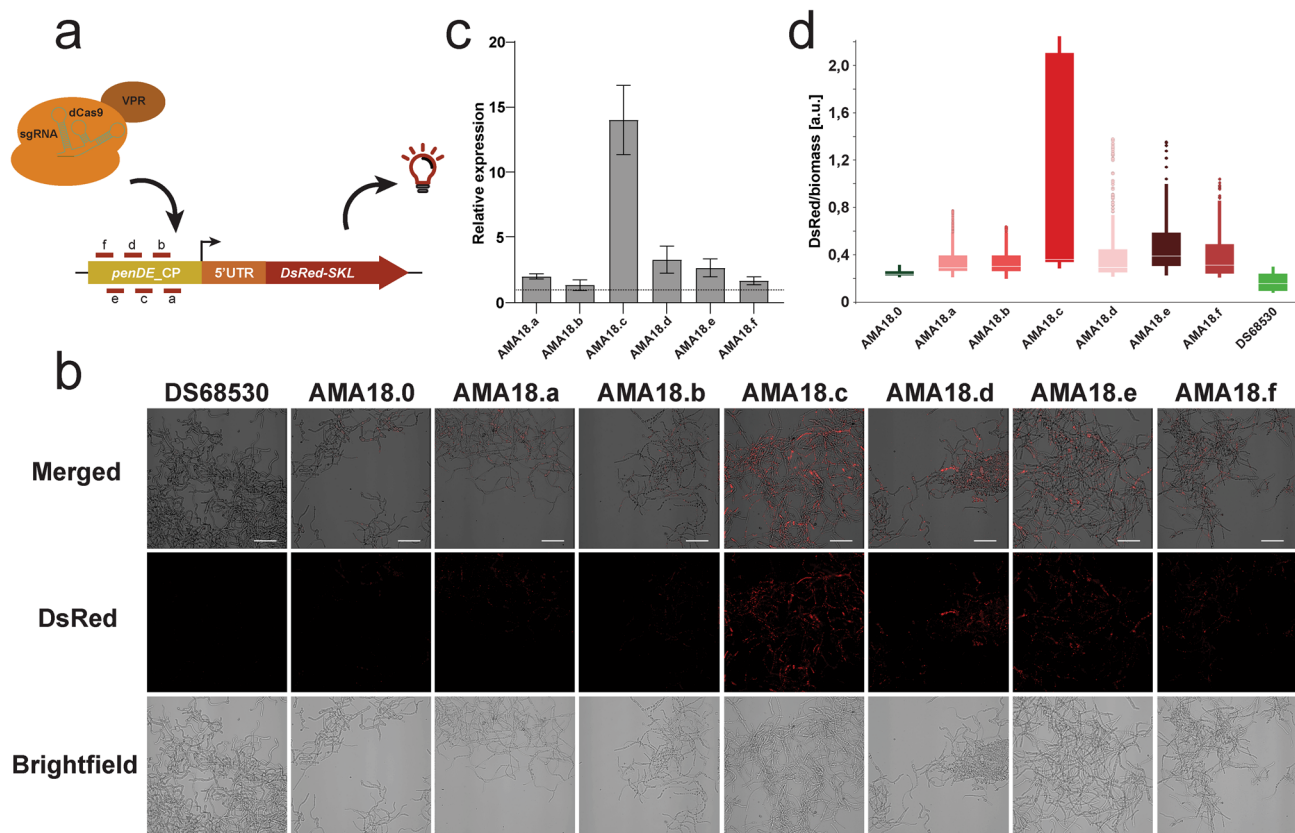


Figure 2. CRISPRa (dCas9-VPR) based activation of *penDE-CP_DsRed*. (a) Schematic representation of the *penDE-CP* upstream *DsRed*. The transcription start site (TSS) is indicated as a black arrow, short lines with letters indicate targeting sites of the sgRNAs. (b) Confocal fluorescence microscopy imaging of *DsRed* targeting CRISPRa strains and controls with no-sgRNA (AMA18.0) and without the *penDE-CP_DsRed* transcription unit (DS68530). Strains were grown for 5 days in liquid SMP media. Scale bars represent 50 μm . (c) qPCR analysis showing expression levels of *DsRed* in CRISPRa strains relative to strain carrying pAMA18.0 no-sgRNA negative control (dotted line) after 5 days of growth in SMP. (d) Development of *DsRed*/biomass over time during time window of 0–40 h cultivation in the BioLector system. Data were obtained from 3 separate experiments, each consisting of 2–3 biological replicates; error bars show the standard deviation.

Fig. S3). The strength of *DsRed* activation by different sgRNAs was determined relative to biomass to avoid variance caused by small differences in growth. During the time interval of 0–40 h, *DsRed*/biomass values in CRISPRa strains were measured and compared to negative control strain carrying pAMA18.0 and the background fluorescence of the DS68530 parental strain. The pAMA18.c carrying strain showed the highest level of relative fluorescence and thus provided the most efficient activation compared to the non-sgRNA negative control (Fig. 2d). All other CRISPRa strains show activation of *penDE-CP_DsRed*, with weakest activation in strains carrying pAMA18.a and pAMA18.b vectors.

CRISPRa-based activation of the transcriptionally silent macrophorin gene cluster. Meroterpenoids represent a large family of natural compounds with diverse biological activities, such as the antimicrobial yanuthones found in *Aspergillus niger*^{37,38}. Highly identical clusters have been found in *Penicillium* species³⁹. These *Penicillium* BGCs contain an additional gene (*macI*), which was shown in *Penicillium terrestre* to encode a terpene cyclase responsible for cyclization of linear yanuthones leading to production of diverse macrophorin analogs³⁹. The putative *P. rubens* macrophorin BGC consists of 11 biosynthetic genes, namely *macA-J* and *macR* as a transcriptional regulator of the cluster (Fig. 3a,b).

Sequence alignment of the provisional sequence of *P. rubens macR* (Pc16g00410) to the *P. terrestre* LM2 *macR* coding sequence (MF989995.1) shows that the *P. rubens macR* sequence is predicted to have an additional intron leading to a premature stop codon. Without this intron, the *P. rubens macR* mRNA should produce a full-length product, similarly to *P. terrestre* LM2 *macR*. To test if *macR* codes for a functional protein we performed promoter replacement in *P. rubens* DS68530, substituting the promoter region of *macR* with the promoter of the *pcbC* (isopenicillin N synthase) gene (Supplementary Fig. S1b), creating strain *macR:OE*. The resulting increase in *macR* transcription (Fig. 3c) led to the activation of the cryptic BGC (Fig. 3d,e) and the production of macrophorins (Fig. 3f,g, Supplementary Table S2). We therefore conclude that *P. rubens macR* encodes for a functional transcription factor and that increased expression of *macR* leads to activation of the entire associated BGC. Moreover, activation of this BGC leads to production of macrophorin-like compounds (Supplementary Table S2).

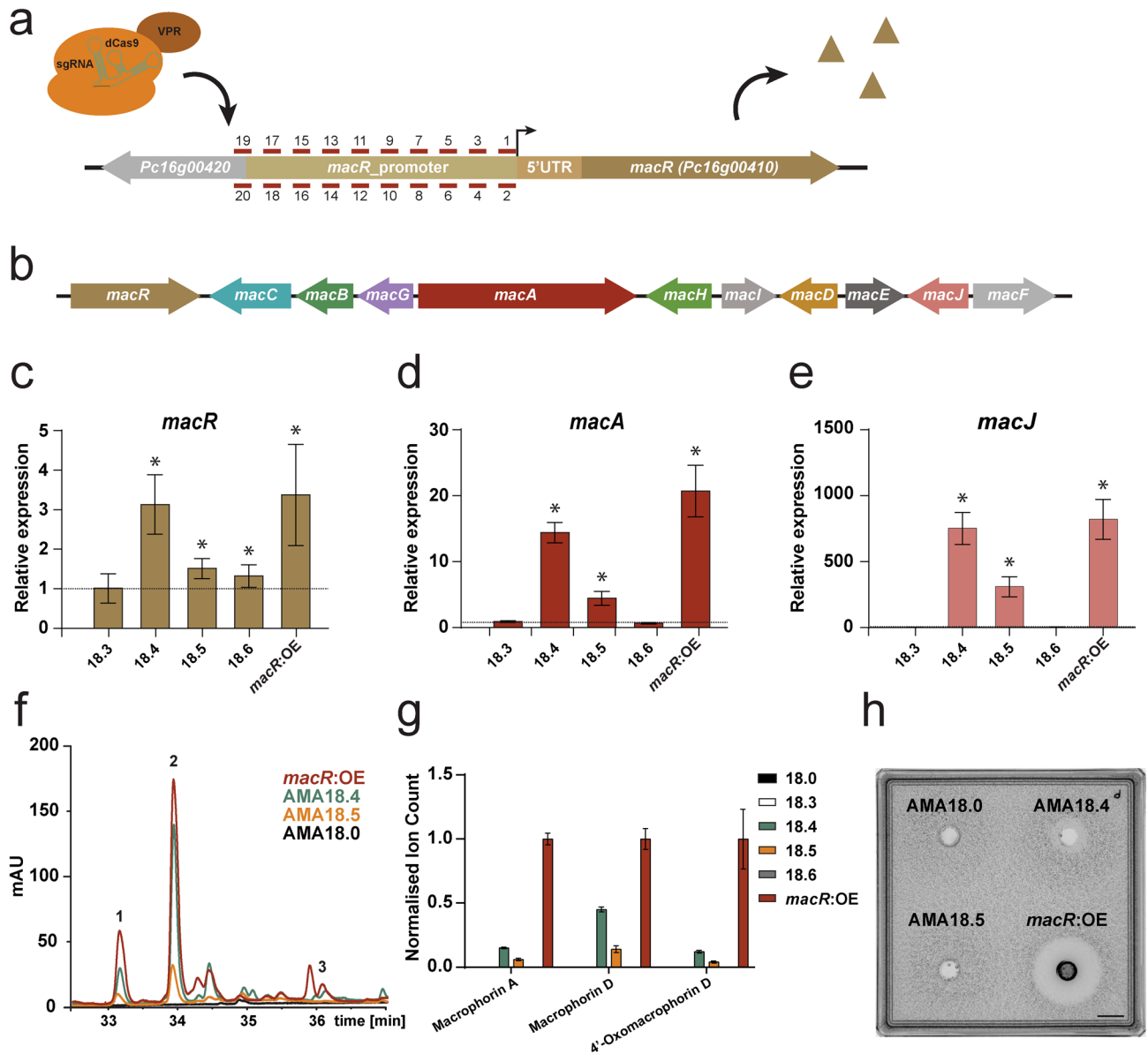


Figure 3. CRISPRa activation of the macrophorin BGC. (a) Schematic representation of the *macR* promoter region. The location of the putative transcription start site (TSS) is indicated as a black arrow, short lines with number indicate sgRNAs targeting sites. (b) Schematic representation of the Macrophorin BGC. qPCR analysis showing expression of *macR* (c) *macA* (d) and *macJ* (e) in the CRISPRa and *macR*:OE strains, relative to the strain carrying the pAMA18.0 vector (non-target control) after 5 days of growth in SMP medium. Error bars indicate the standard error of the mean of three biological replicates with two technical duplicates, and (*) indicates significant up-regulation (Student's-test p-value < 0.05). (f) LC-MS UV-VIS chromatogram ($\lambda = 700$ nm) of hyphae extracts of CRISPRa and *macR*:OE strains representing macrophorin A (1), macrophorin D (2) and 4'-oxomacrophorin D (3). (g) LC-MS analysis of Macrophorin related compounds in hyphae extracts of CRISPRa and *macR*:OE strains. Error bars indicate the standard error of the mean of three biological replicates with two technical duplicates. (h) Bioassay to detect (macrophorin related) antimicrobial activity against *Micrococcus luteus* in the supernatant of indicated strains grown for 5 days in liquid SMP medium. The supernatant was concentrated 10-times and 100 μ l was loaded in a well in top agar containing *M. luteus* at $OD_{600} = 0.0125$. Scale bar represents 10 mm.

Sanger sequencing data of cDNA obtained from the *macR*:OE strain showed 2 introns in *P. rubens macR* mRNA and no pre-mature stop codon, in line with the coding sequence of *macR* of *P. terrestris* (MF989995.1) and the homologous *yanR* (ASPNIIDRAFT_44961) of *A. niger*. It therefore seems likely that the third intron in the provisional *P. rubens macR* sequence is wrongly predicted, and *P. rubens* is capable of producing, not only functional, but also full-length MacR. Additionally, a mutation (cDNA 2611C>T, P776S) mutation was identified in the ORF of *macR*. The effect of this mutation was not further investigated as *macR* remained capable of transcriptional activation. The sequence of *P. rubens* DS68530 *macR* cDNA can be found in Supplementary Note S1.

Since the *P. rubens* macrophorin BGC is silent under our growth conditions (Secondary Metabolite Producing [SMP] medium, 25 °C)^{40,41}, it was selected for activation by CRISPRa. As no TSS is known for *macR*, 20 sgRNAs (*MacR*-sgRNA_1-20) were designed to target the entire 547 bp long, native promoter (Fig. 3a, Supplementary Table S1, Supplementary Fig. S2b). The *macR* targeting CRISPRa strains and the *macR*:OE positive control, were grown on SMP-agar for 10 days after which secondary metabolites were extracted from representative agar plugs, and analyzed by LC-MS (Supplementary Table S3). As expected, no macrophorin production was observed in the strain carrying the pAMA18.0 negative control with no sgRNA insert. Strains expressing *MacR*-sgRNA_4 and *MacR*-sgRNA_5 showed production of compounds with masses corresponding to macrophorin A (361.24 m/z [M + H]⁺), macrophorin D (505.28 m/z [M + H]⁺) and 4'-oxomacrophorin D (503.26 m/z [M + H]⁺) (Supplementary Table S2). None of the other CRISPRa strains exhibited macrophorin production.

Fungal strains carrying vector pAMA18.3–6 and pAMA18.0 (no sgRNA control) were further investigated by qPCR (Fig. 3c–e) and metabolite profiling (Fig. 3f,g). Strains expressing *MacR*-sgRNA_4 and sgRNA_5 were selected as these sgRNAs showed activated macrophorin production (Supplementary Table S3). Although strains carrying *MacR*-sgRNA_3 and sgRNA_6 did not show macrophorin production these strains were also investigated further, as these sgRNAs target the *macR* promoter region in close proximity to the successfully activating *MacR*-sgRNA_4 and sgRNA_5, but on the opposite strand of the DNA. As expected, strains carrying the pAMA18.4 or pAMA18.5 CRISPRa vector showed an increase in *macR* expression compared to the pAMA18.0 control, further confirming CRISPRa dependent transcriptional activation (Fig. 3c). The increase in *macR* expression resulted in transcriptional activation of the macrophorin BGC as exemplified by increased levels of *macA* (polyketide synthase) (Fig. 3d) and *macJ* (proposed terpene cyclase³⁹) mRNA (Fig. 3e), that respectively encode the first and last enzymes in the macrophorin biosynthesis pathway³⁹.

In the strain carrying the pAMA18.4 vector, levels of transcriptional activation were comparable to those in the positive control *macR*:OE while strain carrying vector pAMA18.5 showed a ~ threefold lower transcription compared to this control, for all genes investigated (Fig. 3c–e). No increased expression of *macR*, *macA* or *macJ* was observed for the strain carrying pAMA18.3. In the strain carrying vector pAMA18.6, a slight upregulation of *macR* was observed but this did not result in induction of *macA* and *macJ* (Fig. 3c–e). In line with this, the strain carrying pAMA18.5 produced lower amounts of the examined macrophorin related metabolites compared to the strain with pAMA18.4 (Fig. 3f,g). However, while qPCR analysis showed similar mRNA levels between the *macR*:OE and pAMA18.4 strains, compound production for macrophorin A and 4'-oxomacrophorin D was lower in AMA18.4 compared to the *macR*:OE strain, reaching 15% and 13% respectively. Strain AMA18.4 reached highest production for macrophorin D at ~ 38% of the ion intensity measured in *macR*:OE.

As the related yanuthones produced by *A. niger* display antimicrobial activity against gram positive bacteria⁴², we analyzed the activity of our macrophorin producing *Penicillium* strains against *Micrococcus luteus* using the agar diffusion method. The transformed parent strain *P. rubens* DS68530 does not contain the penicillin BGC, and consequently does not produce compounds inhibiting the growth of *M. luteus*. We observed a clearance zone around concentrated supernatant from the *macR*:OE strain grown for 5 days in SMP medium, and to a lesser extent also around that of the AMA18.4 strain, but not that of the control (AMA18.0) or the AMA18.5 strain (Fig. 3h). This indicates that the macrophorins produced by *P. rubens* are indeed bioactive against Gram-positive bacteria, and CRISPRa dependent activation of the BGC is sufficient to induce antimicrobial activity.

Interestingly, we observed a dark brownish pigmentation of the hyphae of the *macR*:OE strain after 5 days of cultivation on R-agar and SMP-agar as well as on day 1 in SMP liquid medium. The strain carrying the CRISPRa vector pAMA18.4 displayed a milder coloration compared to the colorless hyphae of the parent strain (Fig. 4). Color formation in these *macR* over-expression strains was not investigated further.

Discussion

In this work, we report the application of dCas9-VPR based CRISPRa in the ascomycetous filamentous fungus *Penicillium rubens*. While *Penicillium* is acclaimed for its production of β-lactam antibiotics, it harbors many more BGCs of which a substantial portion remain uncharacterized⁴³. CRISPRa systems have been established in many model organisms as an ideal technology for transcriptional regulation and could aid in activating these often silent BGCs to facilitate characterization.

In our approach dCas9-VPR and the sgRNA are episomally encoded on the same AMA1-based vector, hence a single transformation with a single vector is enough to establish CRISPR-based transcriptional activation in *Penicillium*, without the need for genome engineering of the host organism. Moreover, because AMA1 supports autonomous vector replication in several filamentous fungal species^{30,31}, and as we use established fungal promoters, terminators, and ribozyme based sgRNA processing, we expect the vector to be transferable to other fungal species. The sgRNA “plug-and-play” module of our CRISPRa vector combines Golden Gate cloning approach with blue/white screening. This allows for convenient cloning of new sgRNAs into the vector, reducing experimental time. This is especially important since general criteria for successful sgRNA design are difficult to define, and empiric testing of sgRNAs for each promoter region of interest remains necessary. Due to the ease of cloning our AMA1 vector, this CRISPRa technology could potentially be implemented in connection with larger scale fungal protoplast transformations using microtiter plates⁴⁴, for example in combination with deploying multiple, separate sgRNA processing vectors in one transformation⁴⁵.

To assess the CRISPRa vector for activation of transcriptionally silent promoter activation, we integrated a *penDE* core promoter driven *DsRed* gene into the penicillin-locus of *P. rubens* DS68530 (Δpenicillin-BGC). This *penDE*-CP was selected because it has been reported previously to be insufficient to express the fluorescent reporter on its own, instead depending on the presence of a synthetic transcription factor³⁶. Fluorescence microscopy showed a clear increase in fluorescence with 3 out of 6 sgRNAs tested, compared to a non-sgRNA expressing control (Fig. 2b). Quantification of fluorescence using a BioLector microbioreactor showed increased

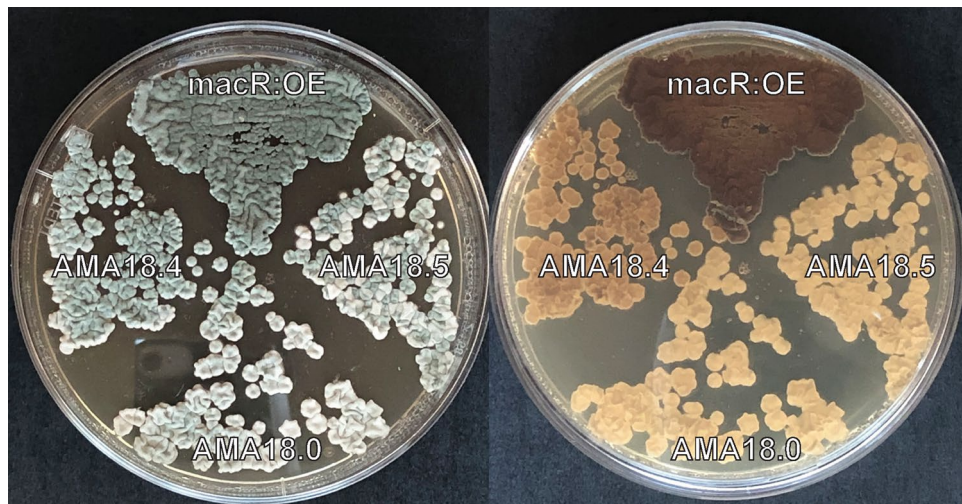


Figure 4. Dark pigmentation of hyphae due to *macR* overexpression in *Penicillium rubens* DS68530 *macR:OE* and in the CRISPRa pAMA18.4 vector carrying strain after 5 days of cultivation on R-agar, compared to AMA18.0 strain carrying pAMA18.0 (no sgRNA) negative control.

fluorescence for 6 out of 6 sgRNA used, showing weak activation for *penDE*-sgRNA_a and *penDE*-sgRNA_b sgRNAs, and, in line with fluorescence microscopy results, *penDE*-sgRNA_c standing out as the most efficient activator (Fig. 2d). The discrepancy between fluorescence microscopy and the BioLector results could possibly be explained by a higher sensitivity of the BioLector, different cultivation method and time points (day 5 of shake-flask cultures for microscopy, average fluorescent during the first 40 h for the BioLector cultivations).

In *A. niger*, Roux and co-workers observed that dCas9-VPR mediated activation of a mCherry fluorescent reporter fused to the transcriptionally silent *Parastagonospora nodorum elcA* promoter was stronger with sgRNAs targeting closer to the start codon, in a window of 162–342 bp upstream of the ATG²⁹. We target a region 106–170 bp upstream the start codon ATG (32–96 bp upstream the TSS) and observe the highest activation with *penDE*-sgRNA_c targeting 129 bp upstream the ATG, and the least with *penDE*-sgRNA_a and _b (not detectable by microscopy) targeting closer to the start codon. We thus do not see the same trend—stronger CRISPRa for sgRNAs targeting closer to the start codon—however we already target a window closer to the ATG compared to Roux et al.²⁹. This exemplifies that it remains difficult to define an optimal targeting conditions, and ideally several sgRNAs should be tested when establishing CRISPRa for a new promoter. In line with what previously was reported for *S. cerevisiae*, we did not observe an effect on CRISPRa efficiency when targeting the plus or minus strand⁴⁶.

To show our CRISPRa system can upregulate an entire silent BGC in *P. rubens* and induce metabolite production, we targeted the *macR* transcription factor of the endogenous macrophorin biosynthesis cluster. Macrophorins are a member of the meroterpenoids, a family of natural compounds which also include, for example, the antimicrobial yanuthones produced by *A. niger*^{37,38}. Homologous macrophorin BGC have been identified in *Penicillium* species, and *P. terrestre* has been shown to produce macrophorins, through the cyclization of yanuthones³⁹. Out of the 20 sgRNAs tested, two resulted in transcriptional activation of the Macrophorin BGC (through the activation of transcriptional factor *macR*) (Fig. 3c,d) and secondary metabolite production (Fig. 3f,g). Although it is impossible to distinguish macrophorins and yanuthones with the method used as they have the same molecular formula, activation of the *macJ* terpene cyclase should lead to cyclic macrophorins³⁹. Additionally we could show that the supernatant of the CRISPRa activated strain grown five days in SMP media exhibited antimicrobial activity against the Gram-positive bacterium *M. luteus* (Fig. 3h). This clearly shows that our dCas9-VPR vector is capable of awakening silent BGCs in *Penicillium* and that the method can aid in product identification and characterization. It should be noted that exchanging the native *macR* promoter with the *pcbC* promoter resulted in higher compound production (Fig. 3g). It might therefore be beneficial to perform promoter exchange for high level production of interesting compounds identified using the CRISPRa technology. A possible explanation for why a larger proportion of the sgRNAs targeting *penDE*-CP (6/6) lead to transcriptional activation compared to *macR* (2/20) may be that the CP is free from most of its native regulatory elements, reducing chances of interference with the binding of the dCas9-VPR regulator. A limiting factor for this way of BGC activation is the need to identify a positive regulator for the cluster, which might not always be known. However, bioinformatics tools like antiSMASH⁴⁷ or CASSIS⁴⁸ could aid by identifying candidate regulators.

Recently, dCas12a (previously Cpf1), from *Lachnospiraceae bacterium* (dLbCas12a) or *Acidaminococcus* sp. (dAsCas12a), has become a popular alternative to dCas9 for gene regulation^{49,50}. The Cas12a system has been popularized due to its ease of multiplexing; dCas12a uses smaller guide RNAs and is capable of processing these from a longer precursor CRISPR RNA⁵¹. Recent literature shows processing of 20 crRNA from a single precursor and simultaneous upregulation of 10 genes by dCas12a fused to a combination of the p65 activation domain together with the heat shock factor 1 in human embryonic kidney (HEK) 293 T cells, exemplifying

the potential of multiplex gene regulation using dCas12a⁵². A potential drawback for using dCas12a in fungi is the low activity at temperatures below 28 °C, while most fungal species grow optimally at temperatures between 25 and 30 °C. However Roux and co-workers recently engineered an temperature tolerant Cas12a mutant (dLbCas12a^{D156R}-VPR), which was successfully employed for CRISPRa mediated gene activation in *A. nidulans* at 25 °C²⁹. While dCas12a is an attractive choice when aiming to upregulate multiple genes simultaneously, for single target activation dCas9-VPR is still a good option. We got significant upregulation of an entire BGC using a single sgRNA targeting the TF of the BGC. For dLbCas12a based upregulation in *A. nidulans* (the unmutated dLbCas12a grown at 37 °C) multiple crRNAs were required for gene activation²⁹. Another consideration when choosing a system is the different PAM requirement, NGG for (d)Cas9 and TTTN for (d)Cas12a. Depending on PAM availability in the genome one or the other could be preferable.

In conclusion we demonstrated that CRISPRa, specifically AMA1 vector-based expression of a dCas9-VPR fusion, can be used for the transcriptional activation of silent BGCs in *P. rubens*. We anticipate that the CRISPRa tool presented here can be widely used to awaken cryptic BGC in filamentous fungal species and thereby aid in the discovery of novel bioactive secondary metabolites.

Methods

Chemicals, reagents and oligodeoxyribonucleotides. All medium components and chemicals were purchased from Sigma-Aldrich (Zwijndrecht, Netherlands) or Merck (Darmstadt, Germany). Oligodeoxyribonucleotide primers (Supplementary Table S4) were obtained from Merck. Enzymes were obtained from Thermo Fisher Scientific (Waltham, MA) unless otherwise stated. For design of nucleic acid constructs, *in-silico* restriction cloning, Gibson Assembly and inspection of Sanger sequencing results, SnapGene (GSL Biotech) was used.

Vector construction. The Golden Gate technology based Modular Cloning (MoClo) system⁵³ using Type IIS BpI and BsaI restriction enzymes were employed for the construction of all vectors unless stated otherwise. Constructed vectors with their destination vectors and corresponding PCR fragments or DNA donor vectors can be found in Supplementary Table S5. PCR amplifications were conducted using KAPA HiFi HotStart ReadyMix (Roche Diagnostic, Switzerland) according to the instructions of the manufacturer. Internal BsaI, BpI recognition sites were removed for MoClo compatibility.

dCas9-2xNLS-VPR was amplified from two different sources. NLS-VPR was amplified from pAG414GPD-dCas9-VPR template (AddGene ID # 63801)¹⁶ and dCas9-NLS was amplified with adding D10A, D839A, H840A and N863A modifications from synthetic spCas9 pYTK036 template, provided as part of the Yeast MoClo Toolkit (AddGene ID # 65143)⁵⁴. DNA sequence of the created dCas9-VPR fusion can be found in Supplementary Note S1a.

The HH and HDV ribozyme based “Plug-and-Play” sgRNA transcription unit was amplified in three parts, where the *gpdA* promoter and the *trpC* terminator together with the HDV self-cleaving sequence were amplified from vector pFC334 (AddGene ID # 87846)³³ and LacZ alpha gene was amplified from the MoClo ToolKit vector pICH41308 (AddGene ID # 47998)⁵³. The promoter of 40S ribosomal protein S8 of *A. nidulans* (AN0465.2, referred to as 40S) and the *tif35* terminator of *P. rubens* Pc22g19890, as well as the transcription unit *penDE*-CP-*DsRed*-SKL-TAct, were amplified from pVE2_10 (AddGene ID #154228)³⁶. The terbinafine selection marker as Pgpda-ergA-TamdS transcription unit was amplified from pCPI_45⁴¹. The promoter of *pcbC* (Pc21g21380, IPNS) was amplified from pVE2_19 (AddGene ID #154241)³⁶, adding 80 bp flanking regions for homologous recombination. The phleomycin selection marker was amplified from pDSM-JAK-109⁵⁵ providing the PpcbC-*ble*-TCYCI transcription unit, adding 80 bp flanking regions for homologous recombination (Supplementary Fig. S1b, Supplementary Table S6).

Our autonomously replicating shuttle vector, carrying the AMA1 sequence, was based on pDSM-JAK-109⁵⁵ where the Pgpda-*DsRed*-SKL-TpenDE transcriptional unit was removed using the BspTI and NotI restriction enzymes. The linear vector was treated with the Klenow Fragment and ligated to the circular vector using the T4 DNA Ligase according to the instructions of the manufacturer, creating a new AMA1 vector without *DsRed* expression. In order to create the CRISPRa vector, this vector was linearized with BspTI and was assembled by Gibson Cloning using PCR fragments G1, G2 G3 (Supplementary Table S5) carrying a terbinafine selection marker, dCas9-VPR and the sgRNA transcription unit respectively. CRISPRa vector pLM-AMA18.0 is deposited to AddGene under ID #138,945. Parallel with this work a catalytically active spCas9 expressing vector was also established (pLM-AMA15.0 AddGene ID #138,944) and utilized for genome editing [manuscript in preparation].

sgRNA target design and cloning. Promoter sequences were analyzed with CCTop⁵⁶ for possible CRISPR RNA guides with the following limitations: protospacer adjacent motif (PAM): NGG, target sequence length 20 bp, core length 12 bp, mismatches taken into account for prediction in core sequence 2, number of total mismatches 4 and using *P. rubens* Wisconsin 54–1255 as the reference genome. Predicted protospacers were manually curated for minimizing off-target effects and selecting high CRISPRater⁵⁷ scores.

Primers were designed to create 89 bp long dsDNA inserts by PCR, containing the unique 20 nt spacer sequence, the hammerhead ribozyme, the 6 bp inverted repeat of the 5'-end of the spacer sequence and the BsaI type II restriction enzyme recognition sites.

For cloning the inserts into the vector pAMA18.0 a modified MoClo protocol⁵³ was used, using FastDigest BsaI (Thermo Fisher Scientific, Waltham, MA) restriction enzyme with an initial 10 min digestion, 50 cycles of digestion and ligation (37 °C for 2 min, 16 °C for 5 min), followed by a final digestion step and a heat inactivation step. Correctly assembled vectors were identified with blue-white screening and confirmed by sequencing. After positive sequence verification and vector extraction, the created pAMA18.X (where X stands for the sgRNA

ID) CRISPRa vector was introduced into the fungal strain of choice (DS68530_ *penDE*-CP_ *DsRed* or DS68530) creating the CRISPRa fungal strain AMA18.X (Fig. 1b, Supplementary Table S6).

Fungal strains and transformation. *P. rubens* strain DS68530⁴⁰ (Δ penicillin-BGC, Δ *hdfA*, derived from DS17690) was kindly provided by Centrient Pharmaceuticals (former DSM Sinochem Pharmaceuticals, Netherlands). Protoplasts of *P. rubens* were obtained 48 h post spore seeding in YGG medium and transformed using the methods and media as described previously¹⁴.

Mycelium was collected by centrifugation at 4000 \times g for 8 min at 4 °C. The pellet was resuspended in 50 ml KC solution (60 g/l KCl; 2 g/l citric acid; pH set to 6.2). After a second round of centrifugation, the pellet was resuspended in 18 ml KC solution and moved to sterile 100 ml shake flask. The mycelium solution was supplemented with 25 mg/ml Glucanex Lysing Enzyme from *Trichoderma harzianum* (Sigma-Aldrich) and incubated at 25 °C and 120 RPM for 90 min. Successful protoplast formation was confirmed by microscopy. Protoplast solution was moved to a sterile falcon tube and was kept on ice when possible. Protoplast were diluted to 50 ml using KC buffer and pelleted by centrifugation at 2770 \times g for 5 min at 4 °C (same settings were used in all subsequent centrifugation steps). Protoplast pellets were resuspended in 25 ml KC buffer followed by addition of 25 ml STC buffer (219 g/l sorbitol, 5.5 g/l CaCl₂, 10 mM Tris-HCl pH 7.5; pH set to 7.5–8.0). After centrifugation, pelleted protoplasts were resuspended in 50 ml STC and counted by microscopy using a counting chamber. After centrifugation protoplasts were resuspended in STC to obtain 2 \times 10⁷ protoplasts/ml (approximately 1–5 ml). These protoplasts were used fresh, or stored at –80 °C in 10% (w/v) PVP-40 (Polyvinylpyrrolidone, Sigma-Aldrich) dissolved in STC as a cryopreservation buffer.

Protoplasts were transformed using PEG-mediated transformation¹⁴. In short, 200 μ l protoplast solution (~2 \times 10⁷ protoplasts/ml) was added to a sterile 12-ml Greiner tube on ice, and were mixed with 1–8 μ g DNA (in maximum 50 μ l) and 200 μ l 20% PEG-4000 solution (33 ml 60% PEG-4000; 67 ml STC buffer; 109.5 g sorbitol; 5 ml 1 M TRIS-HCl buffer pH 7.5; in final volume of 250 ml). Protoplasts were incubated on ice for 30 min. Tubes were supplemented with 1.5 ml 60% PEG-4000 solution (60 g PEG-4000 dissolved in 40 ml H₂O) by heating in a microwave, 1.0 ml 1 M Tris-HCl pH 7.5; 5.0 ml 1 M CaCl₂ in a total volume of 100 ml) and were homogenized completely by rotating the tube for 2 min. The tubes were placed in a 25 °C incubator for 25 min. 1.2 M sorbitol was added to a total of 11 ml, and protoplasts were pelleted by centrifugation at 2770 \times g for 5 min at 25 °C. Protoplasts were carefully resuspended in 1 ml 1.2 M sorbitol and 100, 200 and 300 μ l was plated on solid transformation medium.

When transforming the CRISPRa AMA1 vectors, total DNA did not exceed 1 μ g. For Cas9-mediated genome editing of *macR*:OE and *penDE*-CP_ *DsRed* strains, the appropriate Cas9 RNP mixtures were added. Using CRISPR/Cas9 ribonucleoprotein (RNP) facilitated co-transformation^{13,36}, marker free DNA was delivered in 10:1 molar ratio compared to the fungal marker, not exceeding 8 μ g total DNA. Synthesized sgRNAs were prepared using MEGAscript T7 Transcription Kit (Thermo Fisher Scientific, Waltham, MA) from PCR generated DNA templates, and the Cas9 protein was overexpressed in *E. coli* T7 Express *lysY* from pET28a/Cas9-Cys (AddGene ID #53,261). For each transformation, separate Cas9 RNP mixtures were formed by mixing 27 μ g Cas9 protein (up to 15 μ l), 4 μ l of synthesized sgRNA; 35 μ l 2 \times STC and 30 μ l 10 \times Cas9 activity buffer (HEPES 4.76 g/l; KCl 11.18 g/l; EDTA 0.029 g/l; MgCl₂ \times 7 H₂O 2.03 g/l; pH set to 7.5; DTT 0.08 g/l).

Media and culture conditions. Solid transformation medium was prepared using SAG solid medium (Sucrose 375 g/l; Agar 15 g/l; Glucose Monohydrate 10 g/l) supplemented, in this order, with 4 ml/l Trace Element Solution⁵⁸, 25.7 ml/l stock solution A; 25.7 ml/l stock solution B and 2.4 ml/l 4 M KOH (where stock solution A contained the following: KCl 28.80 g/l; KH₂PO₄ 60.8 g/l; NaNO₃ 240 g/l, at pH 5.5 (adjusted using KOH) and stock solution B contained: MgSO₄·7H₂O at 20.80 g/l). Selection for the terbinafine marker based *macR*:OE cassette and all CRISPRa vector carrying transformants was carried out using 1.1 μ g/ml terbinafine hydrochloride (Sigma-Aldrich) in the solid transformation medium. Terbinafine was supplemented in all media of consecutive experiments, whereas selection for *penDE*-CP_ *DsRed* and *PpcbC-ble-tCYC1* co-transformation was done using medium containing 50 μ g/ml phleomycin (Invivogen, San Diego, CA). For each strain, 2 separate transformant colonies were selected as replicates and re-streaked individually on solid R-agar (see below) medium and cultivated for 7 days on 25 °C to produce spores, which were immobilized on lyophilized rice grains and used for further experiments. Schematic representation of engineering DS68530_ *penDE*-CP_ *DsRed* and *macR*:OE control strains, using CRISPR/Cas9 mediated homologous recombination-based co-transformation into DS68530, is shown on Supplementary Figure S1. For each created strain, transformed DNA is listed in Supplementary Table S6.

For shake-flask liquid cultures, spores immobilized on lyophilized rice grains (0.2 \times 10⁶–2 \times 10⁶ spores/ml) were precultured for 24 h in YGG medium⁵⁹ before inoculation (1:7.5) into 30 ml Secondary Metabolite Producing (SMP) medium⁵⁹ (Penicillin Producing Medium-PPM-without supplemented phenoxyacetic acid or phenylacetic acid), supplemented with 1.1 μ g/ml terbinafine. Cultures were grown at 25 °C in a rotary incubator at 200 RPM for 5 days, after which mycelium was collected for total RNA extraction as well as extraction of secondary metabolites by vacuum filtration over filter paper. Solid R-agar medium⁵⁸ was used for sporulation, SMP-agar (SMP medium supplemented with 15 g/l agar-agar) was used for cultivation, and for secondary metabolite extraction. All solid agar cultures were incubated at 25 °C.

Total RNA extraction and cDNA synthesis. Total RNA was extracted from mycelium collected from cultures grown in SMP for 5 days at 25 °C. Wet biomass (~200 mg) was added to a screw cap tube containing 900 μ l Trizol reagent (Thermo Fisher Scientific, Waltham, MA), 125 μ l chloroform and glass beads (ϕ 0.75–1 mm, 500–600 mg). The samples were stored at –80 °C until RNA isolation. The mycelium was disrupted

using the FastPrep FP120 system (Qbiogene, Carlsbad, CA), followed by total RNA isolation using the phenol-chloroform extraction method. In short, after cell disruption phases were separated by centrifugation (10 min at 14,000×g, the upper phase was transferred to a new tube, followed by a chloroform extraction step (phase separation: 5 min at 12,000×g). RNA was precipitated by the addition of 1 volume isopropanol and incubated on ice for at least 10 min, followed by centrifugation (10 min at 12,000×g). Finally, the RNA was resuspended in milliQ H₂O. DNase treatment was done using the TURBO DNA-free Kit (Thermo Fisher Scientific, Waltham, MA), and the RNA concentration was determined using Nanodrop. cDNA was synthesized using RevertAid H Minus First Strand cDNA synthesis kit (Thermo Fisher Scientific, Waltham, MA) according to the manufacturer's instructions for highly structured mRNAs using oligo (dT)₁₈ primers and 1 µg of total RNA as template in a 20 µl reaction.

qPCR analysis. Primers used to analyze expression *DsRed*, *macR*, *macA* and *macJ* can be found in Supplementary Table S7. Primers were, when possible, designed to overlap an intron–exon junction to avoid amplification on gDNA. The *γ-actin* gene (*Pc20g11630*) was used as a control for normalization. The 25 µl qPCR reaction contained 4 µl of a 20× diluted cDNA synthesis reaction, 0.6 µM each of forward and reverse primer, and 12.5 µl SensiMix SYBR Hi-ROX master mix (Meridian Bioscience, Memphis, TN). Expression levels were determined with a MiniOpticon system (Bio-Rad, Hercules, CA) using the Bio-Rad CFX manager software, the threshold cycle (*Ct*) values were determined automatically by regression. Thermocycler conditions were as follows: 95 °C for 10 min, followed by 40 cycles of 95 °C for 15 s, 60 °C for 30 s, and 72 °C for 30 s. Thereafter, a melting curve was generated to determine the specificity of the qPCRs.

LC–MS sample preparation. For secondary metabolite analysis samples were taken from vacuum filtered mycelium or from solid SMP-agar medium as 3 × 1 cm diameter plugs. The plugs were transferred to a 4.0 ml glass vial and 1 ml acetone supplemented with 4 µl *n*-Dodecyl-β-D-maltoside (DDM) (10 mg/ml in methanol) was added as internal standard. The plugs were extracted ultrasonically for 60 min, after which the extracts were transferred to a clean vial and dried under a nitrogen stream at 25 °C. Dried extracts were resuspended in 200 µl methanol:milliQ-H₂O (1:1) and filtered via a 0.2 µm PTFE syringe filter before the used for LC–MS analysis.

LC–MS metabolite analysis. Metabolite analysis was performed using an Accella1250 UHPLC system coupled to a benchtop ESI–MS Orbitrap Exactive (Thermo Fisher Scientific, Waltham, MA) mass-spectrometer. A sample of 5 µl was injected onto a Waters Acquity CSH C18 UPLC (UHPLC) column (150 × 2.1 mm, 1.7 µm particle size) operating at 40 °C with a flow rate of 300 µl/min. Separation of the compounds was achieved by using a water-acetonitrile gradient system starting from 90% of solvent A (milliQ-water) and 5% solvent B (100% acetonitrile). 5% of solvent C (2% formic acid) was continuously added to maintain a final concentration of 0.1% of formic acid in the mobile phase. After 5 min of initial isocratic flow, the first linear gradient reached 60% of B at 30 min, and the second 95% of B at 35 min. A purge step for 10 min at 90% of B was followed by column equilibration for 15 min at the initial conditions. The column eluent was directed to a HESI-II ion source attached to the Exactive Orbitrap mass spectrometer operating at the scan range (*m/z* 80–1600 Da) and alternating between positive/negative polarity modes for each scan. LC–MS data were analyzed using the Thermo Scientific Xcalibur 2.2 processing software by applying the Genesis algorithm for peak detection and manual integration on the sum of the whole spectra of selected ions. The extracted ion counts of investigated compounds were normalized to the DDM internal standard and represented relative to the average detected values from the *MacR*:OE strain replicates. In addition to LC–MS only UV–VIS absorption was monitored at 220, 354 and 700 nm. Ions corresponding to the $[M + H]^+$ pseudo molecular ions of the final steps of the macrophorin biosynthesis pathway (Macrophorin A, macrophorin D and 4'-oxomacrophorin D) were identified in chromatographic peaks (1), (2) and (3) respectively and were selected for further analysis. The peaks recorded by each channel for (1), (2) and (3) in match in retention time. The chromatogram recorded at 700 nm showed the best signal-to-noise ratio. (Fig. 3f, Supplementary Fig. S4). Due to the necessity of adding an in-line UV–VIS detector between the MS and the column to generate UV–VIS chromatograms, small discrepancy in *Rt* between different datasets was observed.

Biolector. Spores (immobilized on 20 rice grains) were used to inoculate 10 ml SMP and cultures were incubated for 48 h in a rotary incubator at 200 rpm and 25 °C. For BioLector analysis and analysis of growth in FlowerPlate (MTP-48-B) wells, this pre-grown mycelium was diluted 8 times in fresh SMP, supplemented with 1.1 µg/ml terbinafine (except for parent strain DS68530). The 1 ml cultures were grown in the BioLector micro-bioreactor system (M2Plabs, Baesweiler, Germany), shaking at 800 rpm at 25 °C. In the BioLector, biomass was measured via scattered light at 620 nm excitation without an emission filter. The fluorescence of *DsRed-SKL* was measured every 30 min with “DsRed I” 550 nm (bandpass: 10 nm) excitation filter and 580 nm (bandpass: 10 nm) emission filter. Data were obtained from 3 separate experiments, each consisting of 2–3 biological replicates. The data obtained from the BioLector experiments were analyzed and presented using the TIBCO Spotfire Software (TIBCO Software Inc., Palo Alto, CA).

Fluorescence microscopy. For visualization of *DsRed-SKL* fluorescent protein, liquid shake-flask cultures were cultivated for 5 days in SMP, and mycelium was collected and re-suspended in phosphate-buffered saline (58 mM Na₂HPO₄; 17 mM NaH₂PO₄; 68 mM NaCl, pH 7.3). Confocal imaging was performed on a Carl Zeiss LSM800 confocal microscope using 20× objective and ZEN 2009 software (Carl Zeiss, Oberkochen, Germany). The *DsRed* signal was visualized by excitation with a 543 nm helium neon laser (Lasos Lasertechnik, Jena, Germany), and emission was detected using a 565 to 615 nm band-pass emission filter⁶⁰.

Bio-assay. Macrophorin producing strains were tested for antimicrobial activity against *Micrococcus luteus* as follows: Supernatant of *P. rubens* strains carrying either the pAMA18.0, pAMA18.4, pAMA18.5 vector and the *macR*:OE strain was collected after 5 days of growth in liquid SMP medium and concentrated 10× in an Eppendorf Concentrator Plus (30 °C, vacuum for aqua solutions setting). An overlay of soft LA-agar (1%) inoculated with *M. luteus* to an OD600 of 0.125 was poured on top of an agar (1%) bottom layer with Oxford Towers (8 × 10 mm) spaced out evenly. The Oxford Towers were removed aseptically and 100 µl of the 10 × concentrated supernatant was loaded in the resulting wells as indicated. The plate was incubated at 30 °C for 24 h before imaging. The experiment was performed in triplicate.

Received: 13 October 2020; Accepted: 21 December 2020

Published online: 13 January 2021

References

- Keller, N. P. Fungal secondary metabolism: Regulation, function and drug discovery. *Nat. Rev. Microbiol.* **17**, 167–180 (2019).
- Kück, U., Bloemendal, S. & Teichert, I. Putting fungi to work: Harvesting a cornucopia of drugs, toxins, and antibiotics. *PLoS Pathog.* **10**, 3–6 (2014).
- Schueffler, A. & Anke, T. Fungal natural products in research and development. *Nat. Prod. Rep.* **31**, 1425–1448 (2014).
- Scharf, D. H., Heinekamp, T. & Brakhage, A. A. Human and plant fungal pathogens: The role of secondary metabolites. *PLoS Pathog.* **10**, 10–12 (2014).
- Medema, M. H. *et al.* antiSMASH: Rapid identification, annotation and analysis of secondary metabolite biosynthesis gene clusters in bacterial and fungal genome sequences. *Nucleic Acids Res.* **39**, W339–W346 (2011).
- Kautsar, S. A. *et al.* MIBiG 2.0: A repository for biosynthetic gene clusters of known function. *Nucleic Acids Res.* **48**, D454–D458 (2019).
- Brakhage, A. A. & Schroeckh, V. Fungal secondary metabolites—strategies to activate silent gene clusters. *Fungal Genet. Biol.* **48**, 15–22 (2011).
- Lim, F. Y., Sanchez, J. F., Wang, C. C. C. & Keller, N. P. Toward awakening cryptic secondary metabolite gene clusters in filamentous fungi. *Meth. Enzymol.* **517**, 303–324 (2012).
- Knott, G. J. & Doudna, J. A. CRISPR-Cas guides the future of genetic engineering. *Science* **361**, 866–869 (2018).
- Pickar-Oliver, A. & Gersbach, C. A. The next generation of CRISPR–Cas technologies and applications. *Nat. Rev. Mol. Cell Biol.* **20**, 490–507 (2019).
- Schuster, M. & Kahmann, R. CRISPR-Cas9 genome editing approaches in filamentous fungi and oomycetes. *Fungal Genet. Biol.* **130**, 43–53 (2019).
- Song, R. *et al.* CRISPR/Cas9 genome editing technology in filamentous fungi: Progress and perspective. *Appl. Microbiol. Biotechnol.* **103**, 6919–6932 (2019).
- Pohl, C., Kiel, J. A. K. W., Driessen, A. J. M., Bovenberg, R. A. L. & Nygård, Y. CRISPR/Cas9 based genome editing of *Penicillium chrysogenum*. *ACS Synth. Biol.* **5**, 754–764 (2016).
- Pohl, C., Mózsik, L., Driessen, A. J. M., Bovenberg, R. A. L. & Nygård, Y. I. Genome editing in *Penicillium chrysogenum* using Cas9 ribonucleoprotein particles. In *Synthetic Biology Methods in Molecular Biology* Vol. 1772 (ed. Braman, J.) 213–232 (Humana Press Inc., Heidelberg, 2018).
- Houbraken, J., Frisvad, J. C. & Samson, R. A. Fleming's penicillin producing strain is not *Penicillium chrysogenum* but *P. rubens*. *IMA Fungus* **2**, 87–95 (2011).
- Chavez, A. *et al.* Highly efficient Cas9-mediated transcriptional programming. *Nat. Methods* **12**, 326–328 (2015).
- Gilbert, L. A. *et al.* CRISPR-mediated modular RNA-guided regulation of transcription in eukaryotes. *Cell* **154**, 442–451 (2013).
- Qi, L. S. *et al.* Repurposing CRISPR as an RNA-guided platform for sequence-specific control of gene expression. *Cell* **152**, 1173–1183 (2013).
- Hilton, I. B. *et al.* Epigenome editing by a CRISPR-Cas9-based acetyltransferase activates genes from promoters and enhancers. *Nat. Biotechnol.* **33**, 510–517 (2015).
- Vojta, A. *et al.* Repurposing the CRISPR-Cas9 system for targeted DNA methylation. *Nucleic Acids Res.* **44**, 5615–5628 (2016).
- Chen, B. *et al.* Dynamic imaging of genomic loci in living human cells by an optimized CRISPR/Cas system. *Cell* **155**, 1479–1491 (2013).
- Gaudelli, N. M. *et al.* Programmable base editing of T to G in genomic DNA without DNA cleavage. *Nature* **551**, 464–471 (2017).
- Brezgin, S., Kostyusheva, A., Kostyushev, D. & Chulanov, V. Dead cas systems: Types, principles, and applications. *Int. J. Mol. Sci.* **20**, 1–26 (2019).
- Xu, X. & Qi, L. S. A CRISPR–dCas toolbox for genetic engineering and synthetic biology. *J. Mol. Biol.* **431**, 34–47 (2019).
- Deaner, M. & Alper, H. S. Systematic testing of enzyme perturbation sensitivities via graded dCas9 modulation in *Saccharomyces cerevisiae*. *Metab. Eng.* **40**, 14–22 (2017).
- Cámara, E., Lenitz, I. & Nygård, Y. A CRISPR activation and interference toolkit for industrial *Saccharomyces cerevisiae* strain KE6-12. *Sci. Rep.* **10**, 14605 (2020).
- Schwartz, C., Curtis, N., Löbs, A.-K. & Wheeldon, I. Multiplexed CRISPR activation of cryptic sugar metabolism enables *Yarrowia lipolytica* growth on cellobiose. *Biotechnol. J.* **13**, 1700584 (2018).
- Román, E., Coman, I., Prieto, D., Alonso-Monge, R. & Pla, J. Implementation of a CRISPR-based system for gene regulation in *Candida albicans*. *mSphere* **4**, e00001-19 (2019).
- Roux, I. *et al.* CRISPR-mediated activation of biosynthetic gene clusters for bioactive molecule discovery in filamentous fungi. *ACS Synth. Biol.* **9**, 1843–1854 (2020).
- Fierro, F., Kosalková, K., Gutiérrez, S. & Martín, J. F. Autonomously replicating plasmids carrying the AMA1 region in *Penicillium chrysogenum*. *Curr. Genet.* **29**, 482–489 (1996).
- Aleksenko, A. & Clutterbuck, A. J. Autonomous plasmid replication in *Aspergillus nidulans* AMA1 and MATE elements. *Fungal Genet. Biol.* **21**, 373–387 (1997).
- Wang, Q. & Coleman, J. J. Progress and challenges: Development and implementation of CRISPR/Cas9 technology in filamentous fungi. *Comput. Struct. Biotechnol. J.* **17**, 761–769 (2019).
- Nødvig, C. S., Nielsen, J. B., Kogle, M. E. & Mortensen, U. H. A CRISPR-Cas9 system for genetic engineering of filamentous fungi. *PLoS One* **10**, e0133085 (2015).
- Gao, Y. & Zhao, Y. Self-processing of ribozyme-flanked RNAs into guide RNAs *in vitro* and *in vivo* for CRISPR-mediated genome editing. *J. Integr. Plant Biol.* **56**, 343–349 (2014).

35. Engler, C., Gruetzner, R., Kandzia, R. & Marillonnet, S. Golden gate shuffling: A one-pot DNA shuffling method based on type IIS restriction enzymes. *PLoS One* **4**, e5553 (2009).
36. Mészáros, L., Büttel, Z., Bovenberg, R. A. L., Driessen, A. J. M. & Nygård, Y. Synthetic control devices for gene regulation in *Penicillium chrysogenum*. *Microb. Cell Fact.* **18**, 203 (2019).
37. Holm, D. K. *et al.* Molecular and chemical characterization of the biosynthesis of the 6-MSA-derived meroterpenoid yanuthone D in *Aspergillus niger*. *Chem. Biol.* **21**, 519–529 (2014).
38. Petersen, L. M. *et al.* Characterization of four new antifungal yanuthones from *Aspergillus niger*. *J. Antibiot. (Tokyo)* **68**, 201–205 (2015).
39. Tang, M. C. *et al.* Late-stage terpene cyclization by an integral membrane cyclase in the biosynthesis of isoprenoid epoxy-cyclohexenone natural products. *Org. Lett.* **19**, 5376–5379 (2017).
40. Salo, O. V. *et al.* Genomic mutational analysis of the impact of the classical strain improvement program on β -lactam producing *Penicillium chrysogenum*. *BMC Genomics* **16**, 937 (2015).
41. Pohl, C. *et al.* A *Penicillium rubens* platform strain for secondary metabolite production. *Sci. Rep.* **10**, 7630 (2020).
42. Bugni, T. S. *et al.* Yanuthones: Novel metabolites from a marine isolate of *Aspergillus niger*. *J. Org. Chem.* **65**, 7195–7200 (2000).
43. Nielsen, J. C. *et al.* Global analysis of biosynthetic gene clusters reveals vast potential of secondary metabolite production in *Penicillium* species. *Nat. Microbiol.* **2**, 17044 (2017).
44. Kuivanen, J., Korja, V., Holmström, S. & Richard, P. Development of microtiter plate scale CRISPR/Cas9 transformation method for *Aspergillus niger* based on in vitro assembled ribonucleoprotein complexes. *Fungal Biol. Biotechnol.* **6**, 3 (2019).
45. Van Leeuwe, T. M. *et al.* Efficient marker free CRISPR/Cas9 genome editing for functional analysis of gene families in filamentous fungi. *Fungal Biol. Biotechnol.* **6**, 13 (2019).
46. Farzadfard, F., Perli, S. D. & Lu, T. K. Tunable and multifunctional eukaryotic transcription factors based on CRISPR/Cas. *ACS Synth. Biol.* **2**, 604–613 (2013).
47. Blin, K. *et al.* AntiSMASH 5.0: Updates to the secondary metabolite genome mining pipeline. *Nucleic Acids Res.* **47**, W81–W87 (2019).
48. Wolf, T., Shelest, V., Nath, N. & Shelest, E. CASSIS and SMIPS: Promoter-based prediction of secondary metabolite gene clusters in eukaryotic genomes. *Bioinformatics* **32**, 1138–1143 (2016).
49. Tak, Y. E. *et al.* Inducible and multiplex gene regulation using CRISPR-Cpf1-based transcription factors. *Nat. Methods* **14**, 1163–1166 (2017).
50. Liu, Y. *et al.* Engineering cell signaling using tunable CRISPR-Cpf1-based transcription factors. *Nat. Commun.* **8**, 1–8 (2017).
51. Fonfara, I., Richter, H., Bratovič, M., Le Rhun, A. & Charpentier, E. The CRISPR-associated DNA-cleaving enzyme Cpf1 also processes precursor CRISPR RNA. *Nature* **532**, 517–521 (2016).
52. Campa, C. C., Weisbach, N. R., Santinha, A. J., Incarnato, D. & Platt, R. J. Multiplexed genome engineering by Cas12a and CRISPR arrays encoded on single transcripts. *Nat. Methods* **16**, 887–893 (2019).
53. Weber, E., Engler, C., Gruetzner, R., Werner, S. & Marillonnet, S. A modular cloning system for standardized assembly of multigene constructs. *PLoS ONE* **6**, e16765 (2011).
54. Lee, M. E., DeLoache, W. C., Cervantes, B. & Dueber, J. E. A highly characterized yeast toolkit for modular multipart assembly. *ACS Synth. Biol.* **4**, 975–986 (2015).
55. Bovenberg R.A.L., Kiel, J. A. K. W., Wenzel, T. J., Los, A. P. Vector-Host system. *World Intellectual. Prop. Organ.* Application number WO/2012/123429 (2012).
56. Stemmer, M., Thumberger, T., del Sol Keyer, M., Wittbrodt, J. & Mateo, J. L. CCTop: An intuitive, flexible and reliable CRISPR/Cas9 target prediction tool. *PLoS One* **10**, e0124633 (2015).
57. Labuhn, M. *et al.* Refined sgRNA efficacy prediction improves large- and small-scale CRISPR-Cas9 applications. *Nucleic Acids Res.* **46**, 1375–1385 (2017).
58. Kovalchuk, A., Weber, S. S., Nijland, J. G., Bovenberg, R. A. L. & Driessen, A. J. M. Fungal ABC transporter deletion and localization analysis. *Methods Mol. Biol.* **835**, 1–16 (2012).
59. Weber, S. S., Polli, F., Boer, R., Bovenberg, R. A. L. & Driessen, A. J. M. Increased penicillin production in *Penicillium chrysogenum* production strains via balanced overexpression of isopenicillin N acyltransferase. *Appl. Environ. Microbiol.* **78**, 7107–7113 (2012).
60. Singh, R. *et al.* *Hansenula polymorpha* Pex37 is a peroxisomal membrane protein required for organelle fission and segregation. *FEBS J.* **287**, 1742–1757 (2020).

Acknowledgements

The authors would like to thank Arjen M. Krikken for the assistance with confocal fluorescence microscopy imaging.

Author contributions

L.M. and M.H. contributed equally to this work. LC–MS analysis was carried out by N.A.W.K. and L.M. BioLector analysis was carried out by Y.N.. L.M. designed the experiments. L.M. and M.H. carried out all other experiments and wrote the manuscript with critical feedback and help from N.A.W.K., R.A.L.B., Y.N., and A.J.M.D.. Y.N., R.A.L.B., and A.J.M.D. conceived the original idea.

Funding

The project leading to this application has received funding from the European Union's Horizon 2020 Research and Innovation Programme under the Marie Skłodowska-Curie grant agreement No. 713482 (ALERT Program). M.H. received funding from the Swedish Research Council [2019–00596]. N.A.W.K. was supported by the Building Blocks of Life programme, which is subsidized by the Netherlands Organization for Scientific Research (NWO) [BBOL.16.010].

Competing interests

The authors declare no competing interests.

Additional information

Supplementary Information The online version contains supplementary material available at <https://doi.org/10.1038/s41598-020-80864-3>.

Correspondence and requests for materials should be addressed to A.J.M.D.

Reprints and permissions information is available at www.nature.com/reprints.

Publisher's note Springer Nature remains neutral with regard to jurisdictional claims in published maps and institutional affiliations.



Open Access This article is licensed under a Creative Commons Attribution 4.0 International License, which permits use, sharing, adaptation, distribution and reproduction in any medium or format, as long as you give appropriate credit to the original author(s) and the source, provide a link to the Creative Commons licence, and indicate if changes were made. The images or other third party material in this article are included in the article's Creative Commons licence, unless indicated otherwise in a credit line to the material. If material is not included in the article's Creative Commons licence and your intended use is not permitted by statutory regulation or exceeds the permitted use, you will need to obtain permission directly from the copyright holder. To view a copy of this licence, visit <http://creativecommons.org/licenses/by/4.0/>.

© The Author(s) 2021, corrected publication 2021